Nanoscale Advances

ROYAL SOCIETY OF CHEMISTRY

PAPER

View Article Online
View Journal | View Issue

Cite this: *Nanoscale Adv.*, 2023, **5**, 3955

Chelate-functionalized magnetic micelles for sequestration of cisplatin†

Kang Du,‡[a] Pan Liao,[b] Shengsong Yang,[a] Dora von Trentini,[a] Kushal Sharma,[c] Xiaorui Shi,[c] Christopher B. Murray,[ad] Daqing Li*[b] and Ivan J. Dmochowski *[a]

Many cancer patients suffer permanent hearing loss due to accumulation of ototoxic cisplatin in the inner ear. In this study, two types of 100 nm magnetic micelles were developed to sequester cisplatin from aqueous solutions, with the goal of eliminating cochlear ototoxins *via* magnetic microsurgery. The micellar surface was quantitatively functionalized with anionic S-rich ligands and the micelle core encapsulated superparamagnetic iron oxide nanoparticles. Exceptionally effective sequestration is demonstrated, with removal of greater than 95 and 50% of solution Pt, by means of centrifugal filtration and magnetic extraction. Attraction between negatively charged micellar surfaces and cationic Pt-species played a critical role and was only partially screened by physiologic salt solution. Importantly, magnetic micelles introduce negligible impact on the integrity of inner ear hair cells, demonstrating excellent biocompatibility. This study showcases successful magnetic sequestration of Pt-based ototoxins using highly applicable nano-micellar materials. More generally, these examples highlight features of the micelle-water interfacial environment that are important in developing nanomaterials for metallo-medicinal applications.

Received 1st May 2023
Accepted 2nd July 2023

DOI: 10.1039/d3na00290j

rsc.li/nanoscale-advances

Introduction

Cisplatin (*cis*-diamminedichloroplatinum, $Pt(NH_3)_2Cl_2$) is the first-line treatment for many types of cancer and is prescribed for 10–20% of all cancer patients.[1] After cisplatin is uptaken by cells, the Cl^- ligands are substituted by water molecules.[2] The resulting diaquated species, $[Pt(NH_3)_2(H_2O)_2]^{2+}$, can interact with redox-active enzymes (mostly through binding to cysteine thiols) to generate reactive oxygen species (ROS);[3] or crosslink purines to prevent DNA transcription and replication in the nucleus.[4] Both paths can induce apoptosis (programmed cell death). In the event of slow renal clearance of cisplatin, normal cells, particularly non-regenerative neurons are damaged, impairing patients' sensory functions. With more patients surviving cancer, combating the cisplatin-induced side effects is an increasingly important challenge.[5]

One of the major side effects of cisplatin-based chemotherapy is ototoxicity. The resulting permanent hearing damage is suffered by at least 50% of patients who receive cisplatin chemotherapy,[6] with pediatric patients being particularly susceptible.[7] Typically administered by intravenous injection, cisplatin is distributed to most organs within hours and excreted through renal clearance within days,[8] which represents the effective time scales of cisplatin chemotherapy. In contrast, the fluid of the inner ear (perilymph) retains cisplatin, up to 10 μM, for months after the completion of treatment. Such passive cochlear accumulation of cisplatin occurs regardless of tumor type. The enclosed cochlear helical structure isolates the perilymph from the general circulatory system and hinders cisplatin excretion.[8] The persistently elevated cisplatin level can result in irreversible damage to auditory structures, including sensory hair cells.[9] One potential mitigation strategy is to develop co-treatment methods that capture and physically remove Pt-based ototoxins from the cochlea. Such post-chemotherapy co-treatment should ideally be applied to the inner ear, where the effects can be isolated.

Many molecules have been explored to target the unwanted distribution of cisplatin. The general strategies are to form stable coordination complexes with Pt, supply reductants to neutralize the cisplatin-related ROS, or a combination of the two.[10] Glutathione (GSH) is a naturally occurring antioxidant responsible for neutralizing ROS. More importantly, the GSH tripeptide forms stable coordination complexes with various metals, including Pt, through its thiol on the central cysteine

[a]*Department of Chemistry, University of Pennsylvania, Philadelphia, PA 19104, USA. E-mail: ivandmo@sas.upenn.edu*

[b]*Department of Otorhinolaryngology, University of Pennsylvania, Philadelphia, PA 19104, USA. E-mail: lidaqing@pennmedicine.upenn.edu*

[c]*Department of Otolaryngology/Head & Neck Surgery, Oregon Health & Science University, Portland, OR 97239, USA*

[d]*Department of Materials Science and Engineering, University of Pennsylvania, Philadelphia, PA 19104, USA*

† Electronic supplementary information (ESI) available. See DOI: https://doi.org/10.1039/d3na00290j

‡ Current address: Department of Chemistry and Biochemistry, California State University San Marcos, San Marcos, CA 92078.

residue. It is estimated that 60% of intracellular cisplatin is bound to endogenous GSH.[11] Therefore, GSH is a natural and promising candidate for cisplatin co-treatment both as a ligand for Pt and as an antioxidant. On the other hand, synthetic soft chelating ligands, such as dithiocarbamate (DTC), which can be synthesized from CS_2 with either primary or secondary amines, also confer high affinity for cisplatin and Pt-containing species.[12,13] In fact, various DTC derivatives have been proposed as chemotherapy co-treatments,[14] and diethyldithiocarbamate has been widely studied as molecular treatment towards cisplatin-related side effects.[15,16] Importantly, being a bidentate chelate, DTC has strong potential to outcompete endogenous anions, cysteine-rich peptides, and protein-related thiols in binding and isolating cisplatin. Despite the advantages of these molecular co-treatments, the common drawback is the lack of an active excretion mechanism. This is particularly crucial for organs that cannot excrete cisplatin effectively, such as the inner ear with a tightly regulated blood-tissue barrier.

Surface-functionalized magnetic micelles[17] have been developed for various biomedical applications such as diagnostic imaging,[18] targeted drug delivery,[19,20] and selective activation therapies.[21] Related micelles have preliminarily been explored as potential co-treatments to address cisplatin-related ototoxicity.[22] The targeted micelles are composed of biocompatible amphiphilic block copolymers with regions of hydrophobic polycaprolactone (PCL) and hydrophilic polyethylene glycol (PEG) groups (Fig. 1a and S1†). The surface-exposed hydrophilic polymer terminus can be functionalized with chelating groups to capture cisplatin. Importantly, superparamagnetic iron oxide nanoparticles (SPIONs) are encapsulated in the hydrophobic core, enabling magnetic steering. The external magnetic field has been demonstrated to direct movement of nanoparticles in small organs within surgical time frames.[23] Such magnetic steering represents a promising strategy to remove Pt-based ototoxin through microsurgery. Magnetic micelles decorated by a diethylester derivative of the glutathione group (Et_2GSH) have been previously shown to sequester cisplatin.[19] This was evidenced by the elevated Pt content of GSH micelles after incubation in cisplatin solutions. However, the reduction in residual Pt in solution was not detectable. It was even a challenge to explore the cause of poor cisplatin sequestration due to the lack of interfacial characterization. There are few viable methods to assess the extent of terminal modification of polymers and the resulting micellar surfaces, which is one of the major challenges in polymer material research.[24] Moreover, specific amide coupling between the terminal carboxylate on the $PCL_{5.2k}$–$PEG_{5.2k}$–COO^- polymer

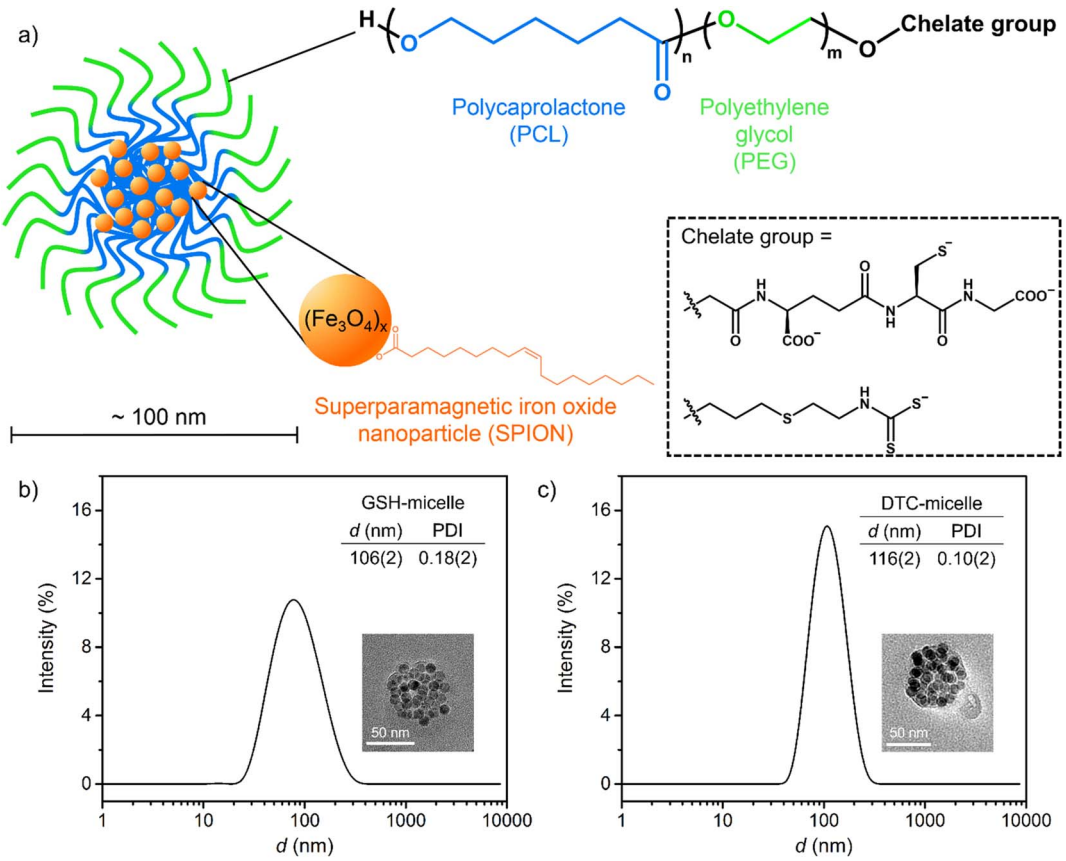

Fig. 1 (a): Chemical structures of components in magnetic micelles. The letters "n" and "m" denote the average molecular weights of PCL and PEG blocks, respectively. Inset: chemical structures for the two chelate groups GSH (top) and DTC (bottom). (b) and (c): Diameter (*d*) distributions of GSH-micelle and DTC-micelle, as measured by DLS experiments. Legends denote the extracted *d* and PDI.

and the amine of GSH necessitated the use of electrostatically neutral Et_2GSH (Fig. S2†), whose affinity for cisplatin is severely impaired due to the lack of electrostatic attraction. As such, viable strategies for magnetic extraction of cisplatin have remained elusive. Highly versatile and effective micelles with exceptional affinity for cisplatin need to be developed.

Herein we report two rationally designed and synthetically versatile micelles that facilitate magnetic sequestration of cisplatin. Micellar surfaces are decorated with anionic GSH or DTC groups. The quantitative end-group functionalization of the PCL–PEG polymers is examined by a suite of molecular site-specific and interfacial-material characterizations. This study demonstrates the applicability of these micelles for chemical isolation and magnetic removal of cisplatin from aqueous solutions. Just as importantly, we identify parameters at the micelle/water interface that govern the overall sequestration performance, such as the Pt binding affinity of the terminal ligands, the overall surface charge of the micelle upon cisplatin binding, and polymer structures that promote SPION encapsulation and micelle magnetic mobilization.

Experimental section

Synthetic procedures

The block copolymers PCL_{5k}–PEG_{5k}–NH_2 and PCL_{5k}–PEG_{5k}–RhB were purchased from Sigma-Aldrich and Nanosoft Polymers, respectively. Pharmaceutical grade cisplatin was supplied by Teva Pharmaceuticals. Full details of SPION synthesis and formation of block copolymers and micelles are provided in ESI.†

Assessment of particle size and surface potential in aqueous solutions

Dynamic light scattering (DLS) and surface potential (ζ potential) experiments were performed on a Zetasizer Nano Z system, with operational software from Malvern Instruments (version 2.0).

^{13}C NMR spectroscopy

^{13}C NMR spectra for all block copolymers were collected on a Bruker DRX 600 instrument with a Bruker Avance DRX console.

Preparation of samples for sequestration studies

For physical filtration, samples were filtered through membranes with 10 kDa cutoff. The average molecular weight of each micelle should greatly exceed 10 kDa, as the molecular weight of a single polymer is already greater than 5 kDa. Therefore, the filtrate was anticipated to be free of Pt-saturated micelles.

For magnetic extraction, samples were placed next to a permanent magnet. After 12 h, micelles congregated at the inner wall of the test tube next to the magnet. The solution was then extracted by careful pipetting. Residual micelles were always visibly present (light brown in solution) due to turbulence and incomplete congregation introduced by pipetting.

Elemental analysis

The quantitation of S, Fe, and Pt elements were carried out by inductively coupled plasma optical emission spectroscopy (ICP-OES), using a Spectro Genesis ICP-OES instrument. Samples were digested and diluted into 3% (v/v) HNO_3 aqueous solutions prior to measurements.

Scanning transmission electron microscopy and energy dispersive spectroscopy (STEM/EDS)

Micelles were characterized by a JEOL F200 transmission electron microscope with a cold field emission source, two large area energy dispersive X-ray spectrometers, and a Gatan One-View IS camera. In a typical experiment, a drop of aqueous solution of micelles was cast onto a carbon-coated copper mesh, which was dried under vacuum for at least 2 h prior to experiments.

Optical spectroscopy

Electronic absorption and fluorescence experiments were carried out on an Agilent Cary 3500 spectrometer and a JASCO FP-8300 spectrofluorometer, respectively.

HEI-OC1 cells

The House Ear Institute-Organ of Corti 1 (HEI-OC1) cells were grown at 33 °C and 10% CO_2 in high-glucose Dulbecco's Modified Eagle's Medium (DMEM) supplemented with 10% fetal bovine serum and 1% penicillin.

Proliferation analysis

The HEI-OC1 cells were used for the *in vitro* cytotoxicity studies in this work due to its advantages of expressing the inner ear biomarkers. The 96-well plate (Falcon) and the microplate readers (Hybrid Multi-Mode Reader, BioTek, USA) were used to culture the HEI-OC1 cells and record the cell number, respectively. The HEI-OC1 cells were first plated with an initial cell number of 3000, and incubated with both micelles containing GSH/DTC at three concentrations—150, 75 and 38 μM. In each well, the total number of cells in a selected region was counted and monitored for 7 consecutive days to quantify the proliferation progress. The number of cells was counted by a microplate reader (Hybrid Multi-Mode Reader, BioTek, USA) and each data point represents the average of three independent experiments.

Imaging for cellular uptake experiments

The HEI-OC1 cells were plated in 8-well plates with seeding density of 1000. After incubation at 33 °C for 24 h, the medium was replaced by micelle-included medium containing 50 μM GSH/DTC. After incubating for 1 h, the cells were imaged using a Zeiss 880 confocal microscope (W-plan-apochromatic 40× lens, 1.0 NA). The serial *Z*-axis confocal images (14 sections with 500 nm *Z* interval) were acquired to locate the optimal *Z*-height for fluorescence signals. The internalized micelles were detected by RhB fluorescence signals with the emission range of 538–599 nm at 514 nm excitation.

Structural analysis of mouse cochlear explant

Matrigel (1 : 10) diluted in Neurobasal medium was incubated in an 8-well chamber slide for 45 min in 37 °C incubator. During this time dissection of the cochlea was carried out in cold HBSS (Hank's blank salt solution). The organ of Corti (P4, C57Bl6) was extracted and transferred to a well containing neurobasal medium. The matrigel was removed from the 8-well chamber slide. The tissue was transferred to each well. 200 μL of control and sample medium (with micelles containing 150 μM GSH) was incubated for 4 d. The media was changed every 2 d. The cilia were first labelled by mouse anti-calretinin (1 : 500), and subsequently stained by goat anti-mouse Alexa Fluor 568 (1 : 1000) before analysis.

Results and discussion

Both new micelle-forming polymers, PCL_{3k}–PEG_{5k}–GSH and PCL_{5k}–PEG_{5k}–DTC (Fig. S1†), can be prepared in one-step substitution reactions and purified by dialysis (Fig. S3 and S4†). The starting polymer PCL_{3k}–PEG_{5k}–CONHS, where the terminal carboxylate is activated as the *N*-hydroxysuccinimide (NHS) ester, reacts selectively with the amine group on GSH. Such pre-activation prevents intramolecular amide formation, preserving the anionic carboxylates on GSH. For the synthesis involving the second polymer, the terminal amine of the starting PCL_{5k}–PEG_{5k}–NH_2, is conveniently and quantitatively converted into a DTC group by reacting with CS_2 in the presence of a base.[25] Notably, attachment of the amine at the terminus of the PEG moiety involves a thioether linkage, which incorporates a single sulfur (S) atom within the polymer. Modifying this polymer with CS_2 should therefore triple the S content. The experimental S content in the synthesized and purified PCL_{3k}–PEG_{5k}–GSH was 0.4%, which is consistent with one S atom in a polymer with an average molecular weight of 8000 g mol^{-1}. Likewise, the S content of the purified PCL_{5k}–PEG_{5k}–DTC polymer was 1.6%, which is exactly 3-fold greater than the PCL_{5k}–PEG_{5k}–NH_2 starting material (%S = 0.52%, Fig. S1 and S4†). These elemental analyses indicated stoichiometric terminal functionalization in both polymers. In addition, ^{13}C NMR spectra revealed clean resonances from both the PCL and PEG regions (Fig. S5 and S6†). Importantly, the consistent ratios of peak integrations between starting material and products confirmed the integrity of both polymers. The identity of the terminal DTC group can be further confirmed by the characteristic carbonyl resonance at −204 ppm,[25] when $^{13}CS_2$ was used in place of $^{12}CS_2$ in the synthesis for PCL_{5k}–PEG_{5k}–DTC (Fig. S6,† inset). Note that both elemental analysis and ^{13}C NMR unambiguously confirm the presence of DTC as terminal groups. Trace amounts of DTC could be further converted to isothiocyanate,[26] which would lower the Pt-binding effectiveness. There is no measurable evidence of isothiocyanate in the present study, but preventative measures can be taken in future studies by utilizing secondary DTC groups.

The preparation of magnetic micelles was improved from literature protocols, in which a toluene solution of polymers and SPION is added to water under sonication (Fig. S7†).[18] Notably, using a highly monodisperse 10 nm SPION sample from an improved protocol[27] resulted in more reproducible and consistent magnetic micelles than the 7 nm ones used previously.[18]

Magnetic micelles made from PCL_{3k}–PEG_{5k}–GSH and PCL_{5k}–PEG_{5k}–DTC, denoted as GSH-micelle and DTC-micelle, have hydrodynamic diameters of 106(2) and 116(2) nm, respectively. Importantly, the polydispersity index (PDI) of both micelles was well below 0.2, demonstrating excellent monodispersity (Fig. 1b and c). Furthermore, spherical clusters (*ca.* 75 nm) of SPIONs were observed in transmission electron micrographs (TEM), which were consistent with the proposed micellar structure, where SPIONs were encapsulated in the hydrophobic core. Note that the diameters of these clusters are less than 100 nm in the micrographs, likely because of the limitation of TEM to image organic polymers, and also the hydration shell of micelles in solution (Fig. 1b and c, inset).[28]

The cisplatin sequestration effectiveness was quantified by residual Pt in solutions treated with micelles, as measured by inductively coupled plasma optical emission spectroscopy (ICP-OES). Solutions of micelles containing 150 μM of either GSH or DTC were incubated with 10 μM cisplatin. After incubation, magnetic micelles were removed by either centrifugal filtration or magnetic extraction. The residual Pt in the collected solutions was then measured to determine the extent of cisplatin sequestration (Fig. 2a).

Cisplatin was effectively removed by either micelle in water (pH = 7, at 37 °C) followed by centrifugal filtration (Fig. 2b and c, data in black). Surprisingly, in the experiment with GSH-micelle, only 5% of residual Pt remained in solution after incubation for 24 h. Such performance represents exceptionally high sequestration effectiveness within a highly applicable surgical timescale. Afterwards, the sequestration process was essentially complete, with no further decrease in residual Pt. This result represents a dramatic improvement over the previously reported Et_2GSH-functionalized micelles. Compared to GSH-micelle, the DTC-micelle removed cisplatin at a slower rate. The residual Pt content dropped to 49% within 24 h, and continued to decrease to 27% after 96 h. It is intriguing that the GSH-micelle significantly outperformed DTC-micelle in water, even though DTC is a bidentate S-rich ligand. We note that the major Pt-containing species in low-chloride solution is cationic $[Pt(NH_3)_2(H_2O)_2]^{2+}$. The highly anionic GSH ligand confers strong electrostatic attraction, in addition to the Pt–S covalent interaction, both of which likely contribute to the excellent cisplatin sequestration. These results represented dramatic improvements over a previous micelle prototype,[18] in which reduction in solution Pt was not detectable. The synthetic versatility of the current micellar constructs enables rational design for efficient Pt sequestration.

To explore the role of cisplatin at the micelle/water interface, the change in micellar surface potential (ζ) was studied upon cisplatin binding. The ζ values measured for GSH- and DTC-micelles (150 μM ligands) were −35.0(4) and −27.5(2) mV in water, respectively, which were consistent with micellar surfaces decorated by anionic ligands. When incubated with 10 μM cisplatin, ζ for both micelles monotonically increased to

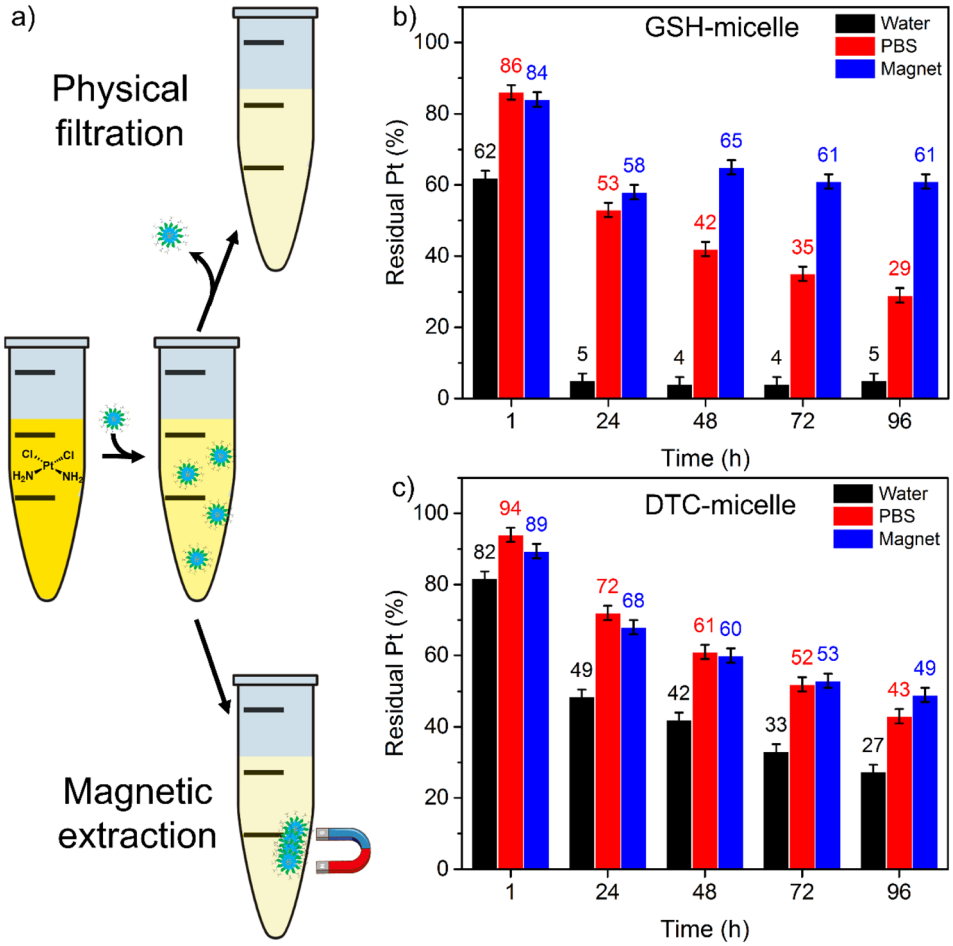

Fig. 2 (a): Demonstration of cisplatin sequestration experiments. (b) and (c): Percentage of residual Pt in solutions treated by GSH-micelles and DTC-micelles, respectively. In each experiment, 10 μM cisplatin was incubated with micelles that contain 150 μM GSH or DTC at pH 7 and 37 °C. Data in black and red represent sequestration experiments in water and PBS, and filtrate solutions were collected for analysis after centrifugal filtration. Data in blue represent sequestration experiments in water followed by magnetic extraction of micelles.

−29.0(9) and −18.8(5) over 96 h (Fig. S8 and S9†). The surface of both micelles became less negative, indicating neutralization by $[Pt(NH_3)_2(H_2O)_2]^{2+}$ binding. To examine further the influence of cisplatin binding on ζ, GSH- and DTC-micelles (20 μM ligands) were incubated with large excess of cisplatin (200 μM). The ζ for both micelles became more positive within 48 h and remained unchanged thereafter (Fig. 3), indicating the expected surface saturation by cisplatin. The ending ζ value after 96 h was

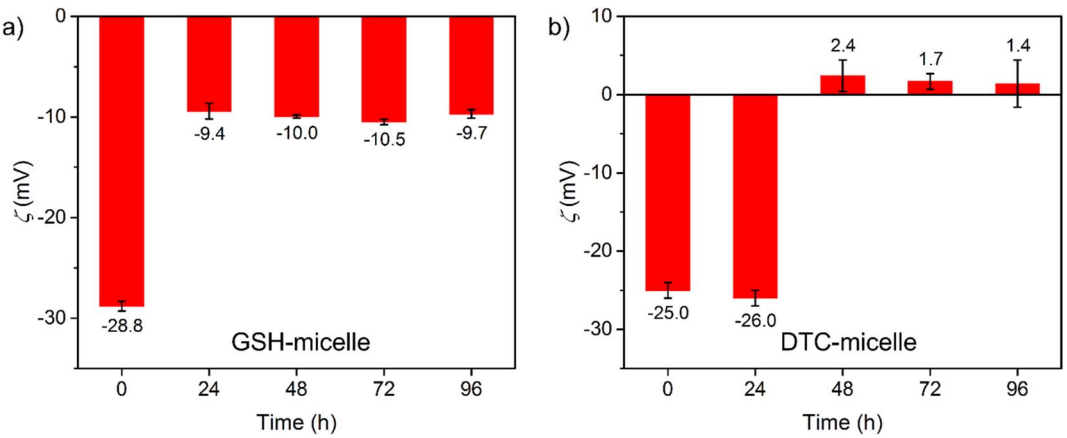

Fig. 3 Progression in ζ of (a) GSH- and (b) DTC-micelles over 96 h, in the presence of cisplatin in H_2O, incubated at 37 °C and pH = 7. The concentrations for chelates and cisplatin were 20 and 200 μM, respectively.

−9.7(8) and 1.4(9) mV for GSH- and DTC-micelles. This significant difference in ζ is in stark contrast to the very similar starting values, −28.8(9) and −25.0(9) mV. The electrostatic neutrality of cisplatin-saturated DTC-micelle suggests that it is not energetically favorable to form a micellar surface fully decorated by cationic $[R–NHCS_2Pt(NH_3)_2]^+$ species, which would otherwise have led to a highly positive ζ. On the other hand, the negative ζ of cisplatin-saturated GSH-micelle further confirms the importance of weakly-or-non-cisplatin-binding carboxylates in conferring strong electrostatic attraction to $[Pt(NH_3)_2(H_2O)_2]^{2+}$. The contrast in ζ and cisplatin sequestration between GSH- and DTC-micelles highlights the importance of designing the chemical environment on the nanoscale, instead of assuming a mere sum of molecular properties.

Pt binding experiments were carried out in phosphate-buffered saline (PBS) to examine influence from Cl^- (150 mM, analogous to blood),[29] which should inhibit the formation of the reactive $[Pt(NH_3)_2(H_2O)_2]^{2+}$ species and cisplatin sequestration (Fig. 2b and c, data in red). Surprisingly, despite $[Cl^-]$ being 1000-fold higher than the surface ligands, both micelles demonstrated appreciable sequestration efficiency. GSH- and DTC-micelles removed 47 and 28% Pt in 24 h, and 71 and 57% at the end of 96 h. Note that the chloride inhibition of GSH-micelle was more severe than in the DTC-micelle. This is likely because the neutral cisplatin molecule is less attracted to the anionic surface than $[Pt(NH_3)_2(H_2O)_2]^{2+}$, while the chelate effect makes the bidentate DTC group more resistant to Cl^- competition.

Finally, the efficiency of magnetic extraction was examined. Permanent magnets were placed next to incubation tubes to congregate the cisplatin-bound micelles. Micelle-excluded solution was extracted *via* careful pipetting and the Pt content was analyzed (Fig. 2b and c, data in blue). Within the first 24 h, GSH-micelle removed over 40% of the Pt, but sequestration remained unchanged with further incubation up to 96 h. In comparison, the DTC-micelle removed over 30% of the Pt in the first 24 h and the extraction of cisplatin continued, with 50% Pt removed at the end of 96 h. Notably, the progressing patterns between filtration and magnetic extraction are very similar for both micelles, despite the difference in residual Pt. Therefore, the lower sequestration effectiveness with magnetic extraction is likely due to incomplete elimination of cisplatin-bound micelles. The eventually more effective magnetic extraction of cisplatin by the DTC-micelle may be attributed to the more stable SPION encapsulation by the larger hydrophobic PCL block (avg. MW of 5k PCL in DTC-micelle *vs.* 3k PCL in GSH-micelle). Block copolymer can self-assemble into micelles only when the MW of PCL is less than the MW of PEG.[30] As such, balancing stable SPION encapsulation with micelle formation must guide the selection of polymers for future applications of magnetic micelles.

To visualize binding of cisplatin to magnetic micelles, elemental distribution of single micelles was mapped by energy dispersive spectroscopy using STEM-EDS. After incubation with excess cisplatin and purification by dialysis, the elemental distribution of a single cisplatin-saturated DTC-micelle was

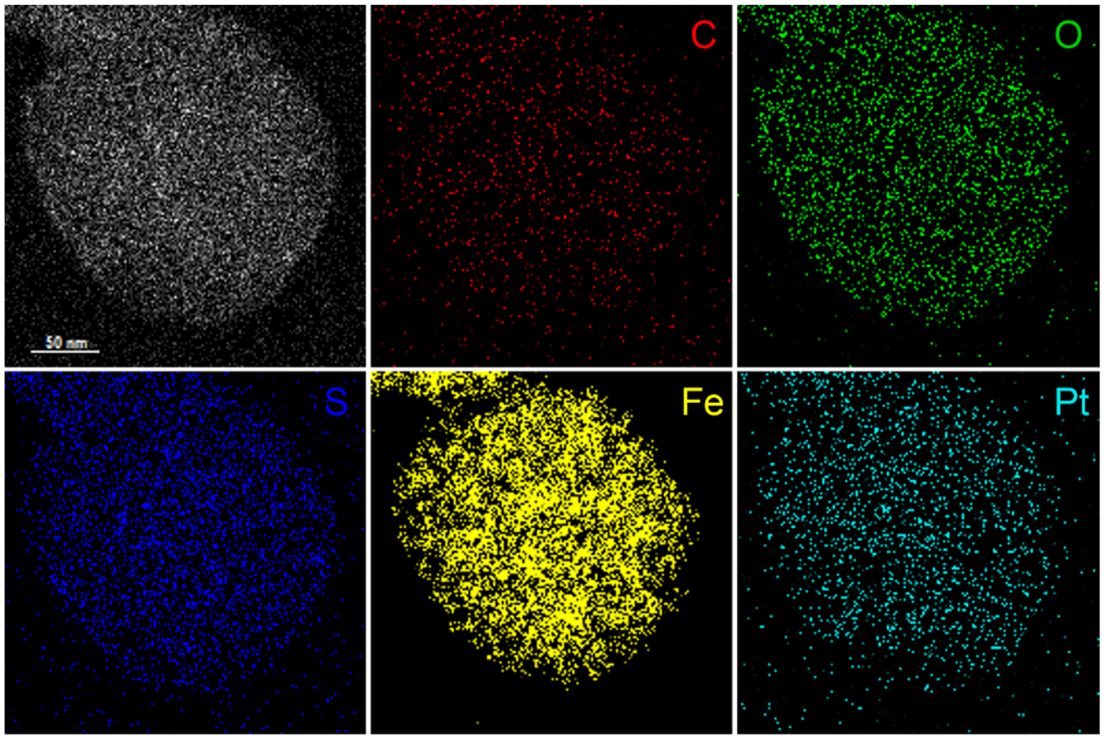

Fig. 4 STEM-EDS elemental maps of a single DTC-micelle, isolated after incubation in cisplatin solution at pH 7 and 37 °C for 2 d. The concentrations for DTC and cisplatin are 20 and 200 μM, respectively, during the incubation. Red, green, blue, yellow, and cyan signals represent characteristic emissions from C, O, S, Fe, and Pt elements, respectively. The scale bar represents 50 nm.

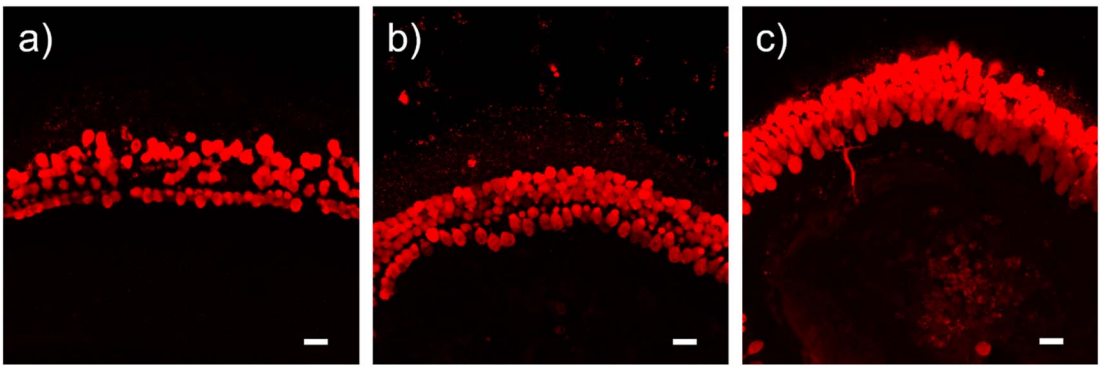

Fig. 5 Fluorescence micrographs of hair cells from mouse cochlear explants incubated with (a) no micelle and with GSH-micelles with GSH concentrations of (b) 150 μM and (c) 75 μM for 4 d. The colored regions represent hair cell cilia stained with calretinin. The scale bar represents 20 μm in each image.

analyzed (Fig. 4). The exclusive element on PCL_{5k}–PEG_{5k}–DTC, S, colocalizes with Fe in SPION, confirming the presumed micellar structure. More importantly, Pt was detected (Fig. 4 and S10†) and colocalized with the above elements, strongly indicating that cisplatin sequestration happened at the micelle/solution interface. Unfortunately, elemental mapping of cisplatin-bound GSH-micelles was not successful due to sample instability under preparation conditions, despite extensive efforts. Note that the experimental conditions involve high vacuum, and a high-voltage electron beam that may damage the GSH-micelle more than DTC-micelle. However, such "instability" in the conditions required for STEM-EDS is not observed in aqueous solution, where solution-state characterizations confirmed the stability of both micellar samples. Nevertheless, the cisplatin-bound GSH-micelle is expected to have a similar structure to its DTC counterpart, based on the above solution-state characterizations.

Nanoparticles are known to be endocytosed by mammalian cells,[31] which motivated the investigation of cellular uptake of GSH- and DTC-micelles. Fluorescently labelled micelles were prepared by doping 1% of Rhodamine B-functionalized (RhB) block copolymer, PCL_{5k}–PEG_{5k}–RhB (structure in Fig. S1†) in the preparations of micelles to give RhB–GSH- and RhB–DTC-micelles (characterizations in Fig. S11–S14†). After 1 h incubation, both micelles were readily uptaken by HEI-OC1 cells (Fig. S15 and S16†), which was chosen as a model due to its expression of many inner ear biomarkers.[32] Such rapid uptake is intriguing, because both the cell membrane and the micellar surface are anticipated to be negatively charged. The implication of cellular uptake of micelles is multifaceted. On one hand, the hydrolyzed $[Pt(NH_3)_2(H_2O)_2]^+$ is the major species in an intracellular environment, which is more susceptible to sequestration by magnetic micelles. On the other, while exosome-assisted excretion of magnetic nanoparticles is not uncommon,[33] a mechanism to promote exocytosis of cisplatin-bound micelles will require further investigation.

Biocompatibility of magnetic micelles was initially evaluated by cell proliferation. When incubated with both micelles, HEI-OC1 cells continued to proliferate, although at a slower rate compared to the control (Fig. S17 and S18†). The pharmacological responses of HEI-OC1 cells are known to be complex.[34] Therefore, the integrity of cochlear explants was applied as a more realistic indicator of biocompatibility.[35] After 4 day incubation with GSH-micelle, the hair cell structures were well preserved (Fig. 5), indicating negligible impact on the integrity of the explants. Importantly, the concentrations of GSH-micelle applied are comparable to those in sequestration experiments. Notably, in future applications designed to limit ototoxicity, surgical introduction and manipulation of magnetic micelles are anticipated to be a much shorter process than incubation in the above biocompatibility experiments. It is likely to employ a higher concentration of micelles, followed by rapid magnetic extraction, for more efficient sequestration of the ototoxin.

Conclusions

The foregoing results demonstrate a successful proof-of-principle strategy for removing cisplatin-based ototoxins from solution using surface-functionalized magnetic micelles. Micelles with two new block copolymers of different lengths were developed *via* quantitative installation of terminal GSH and DTC ligands. Both polymers are capable of self-assembling into *ca.* 100 nm magnetic micelles. Surface potential characterization demonstrated that the micellar surfaces are negatively charged and are neutralized upon binding cisplatin and its hydrolyzed products. Trianionic GSH confers advantages by neutralizing the build-up of positive charge that occurs when cisplatin binds the micellar surface. Both GSH- and DTC-micelles exhibit effective and efficient sequestration of cisplatin in solution with up to 95% cisplatin removal by physical filtration, and successful competition with endogenous Cl^-. Furthermore, magnetic sequestration is successfully demonstrated to remove over 50% of cisplatin from aqueous solutions, with use of permanent magnets. Further optimization of the micellar system will integrate surface groups with a high degree of negative charge and high molecular Pt-binding affinity. Finally, these micelles exhibit intriguing biological properties. They are rapidly uptaken by mammalian cells even at low concentrations. Concentration-dependent inhibition of

cell proliferation is observed for both micelles, but they have negligible influence on the structural integrity of cochlear hair cells.

Building upon these results, sequestration of Pt-based ototoxins will be evaluated in an animal model of cisplatin-induced ototoxicity,[35,36] with the eventual goal of developing non-invasive local approaches that sequester cisplatin in an active and controllable manner. Such approaches will involve micelle introduction through the oval window of cochlea, sound-triggered steering of the micelles to follow the flow of perilymph, and magnetic collection of the Pt-bound micelles at the round window. A nanohydrogel formulation will promote delivery of SPION-micelles to the cochlea of the inner ear.[32–37] Cisplatin-induced ototoxicity will be evaluated with the mouse model, using molecular markers and auditory brainstem response (ABR) test to quantify any hearing restoration, following SPION-micelle inner ear delivery.[36–39]

This study also highlights some of the design considerations for physical–chemical tuning of nanosystems, such as the electrostatic environment at the nanoparticle-micelle surface, which goes beyond the molecular properties of the individual surface ligands. The knowledge gained from the current study points to an ideal nano-construct, in which the micellar surface has both non-cisplatin-binding anionic groups and high-affinity multidentate chelates.

Author contributions

The manuscript was written with contributions of all authors. All authors have given approval to the final version of the manuscript. KD and PL contributed equally.

Conflicts of interest

There are no conflicts to declare.

Acknowledgements

This work was supported by NIH grant R35-GM-131907 to IJD, NIH grant R01-DC-017144 to DL, Office of Naval Research Multidisciplinary University Research Initiative Award ONR N00014-18-1-2497 to CBM and SY, and NIH/NIDCD grant R01-DC010844 to XS. KD was supported by the University of Pennsylvania. We thank Drs David R. Vann for assistance with ICP-OES and Douglas Yates for STEM-EDS experiments, with support from the UPenn MRSEC, DMR-1720530.

References

1 L. Kelland, *Nat. Rev. Cancer*, 2007, **7**, 573–584.
2 D. Wang and S. J. Lippard, *Nat. Rev. Drug Discovery*, 2005, **4**, 307–320.
3 A. Mandic, J. Hansson, S. Linder and M. C. Shoshan, *J. Biol. Chem.*, 2003, **278**, 9100–9106.
4 P. M. Takahara, A. C. Rosenzweig, C. A. Frederick and S. J. Lippard, *Nature*, 1995, **377**, 649–652.
5 R. Oun, Y. E. Moussa and N. J. Wheate, *Dalton Trans.*, 2018, **47**, 6645–6653.
6 A. Callejo, L. Sedó-Cabezón, I. Domènech Juan and J. Llorens, *Toxics*, 2015, **3**, 268–293.
7 Y. Li, R. B. Womer and J. H. Silber, *Eur. J. Cancer*, 2004, **40**, 2445–2451.
8 A. M. Breglio, A. E. Rusheen, E. D. Shide, K. A. Fernandez, K. K. Spielbauer, K. M. McLachlin, M. D. Hall, L. Amable and L. L. Cunningham, *Nat. Commun.*, 2017, **8**, 1654.
9 M. W. M. van Ruijven, J. C. M. J. de Groot and G. F. Smoorenburg, *Hear. Res.*, 2004, **197**, 44–54.
10 L. P. Rybak, D. Mukherjea, S. Jajoo and V. Ramkumar, *Tohoku J. Exp. Med.*, 2009, **219**, 177–186.
11 T. Ishikawa and F. Ali-Osman, *J. Biol. Chem.*, 1993, **268**, 20116–20125.
12 C. C. Hadjikostas, G. A. Katsoulos and S. K. Shakhatreh, *Inorg. Chim. Acta*, 1987, **133**, 129–132.
13 G. Hogarth, *Mini-Rev. Med. Chem.*, 2012, **12**, 1202–1215.
14 Y. Ge, N. Zheng, X. Chen, J. Zhu, W. Sun, J. R. Olson, D. S. Aga, W. Hu, X. Tang and X. Ren, *Chem. Res. Toxicol.*, 2019, **32**, 1572–1582.
15 J. M. Berry, C. Jacobs, B. Sikic, J. Halsey and R. F. Borch, *J. Clin. Oncol.*, 1990, **8**, 1585–1590.
16 S. M. Somani, R. Ravi and L. P. Rybak, *Drug Chem. Toxicol.*, 1995, **18**, 151–170.
17 L. E. Euliss, S. G. Grancharov, S. O'Brien, T. J. Deming, G. D. Stucky, C. B. Murray and G. A. Held, *Nano Lett.*, 2003, **3**, 1489–1493.
18 J. Lu, S. Ma, J. Sun, C. Xia, C. Liu, Z. Wang, X. Zhao, F. Gao, Q. Gong, B. Song, X. Shuai, H. Ai and Z. Gu, *Biomaterials*, 2009, **30**, 2919–2928.
19 T.-M. Sun, J.-Z. Du, Y.-D. Yao, C.-Q. Mao, S. Dou, S.-Y. Huang, P.-Z. Zhang, K. W. Leong, E.-W. Song and J. Wang, *ACS Nano*, 2011, **5**, 1483–1494.
20 G. Yeroslavsky, M. Richman, A. Gertler, H. Y. Cohen, M. Motiei, R. Popovtzer, H. E. Gottlieb and S. Rahimipour, *ACS Appl. Nano Mater.*, 2021, **4**, 14126–14135.
21 L. Yan, A. Amirshaghaghi, D. Huang, J. Miller, J. M. Stein, T. M. Busch, Z. Cheng and A. Tsourkas, *Adv. Funct. Mater.*, 2018, **28**, 1707030.
22 M. N. Kayyali, A. J. Ramsey, E. M. Higbee-Dempsey, L. Yan, B. W. O'Malley Jr, A. Tsourkas and D. Li, *J. Assoc. Res. Otolaryngol.*, 2018, **19**, 123–132.
23 E. J. Snider, K. P. Kubelick, K. Tweed, R. K. Kim, Y. Li, K. Gao, A. T. Read, S. Emelianov and C. R. Ethier, *Sci. Rep.*, 2018, **8**, 12251.
24 S. P. O. Danielsen, H. K. Beech, S. Wang, B. M. El-Zaatari, X. Wang, L. Sapir, T. Ouchi, Z. Wang, P. N. Johnson, Y. Hu, D. J. Lundberg, G. Stoychev, S. L. Craig, J. A. Johnson, J. A. Kalow, B. D. Olsen and M. Rubinstein, *Chem. Rev.*, 2021, **121**, 5042–5092.
25 M. Imran, Z. ur-Rehman, G. Hogarth, D. A. Tocher, G.-S. Chaudhry, I. S. Butler, F. Bélanger-Gariepy and T. Kondratyuk, *Dalton Trans.*, 2020, **49**, 15385–15396.
26 K. Eschliman and S. H. Bossman, *Synthesis*, 2019, **51**, 1746–1752.

27 L. Qiao, Z. Fu, J. Li, J. Ghosen, M. Zeng, J. Stebbins, P. N. Prasad and M. T. Swihart, *ACS Nano*, 2017, **11**, 6370–6381.
28 B. Kuei and E. D. Gomez, *Microsc. Microanal.*, 2018, **24**, 1988–1989.
29 Q. J. Wan, P. Kubáň, J. Tanyanyiwa, A. Rainelli and P. C. Hauser, *Anal. Chim. Acta*, 2004, **525**, 11–16.
30 K. Letchford and H. Burt, *Eur. J. Pharm. Biopharm.*, 2007, **65**, 259–269.
31 N. Oh and J.-H. Park, *Int. J. Nanomed.*, 2014, **9**, 51–63.
32 P. Devarajan, M. Savoca, M. P. Castaneda, M. S. Park, N. Esteban-Cruciani, G. Kalinec and F. Kalinec, *Hear. Res.*, 2002, **174**, 45–54.
33 Y. Chen and S. Hou, *Stem Cell Res. Ther.*, 2022, **13**, 135.
34 G. Kalinec, P. Thein, C. Park and F. Kalinec, *Hear. Res.*, 2016, **335**, 105–117.
35 R. M. Cardinaal, J. C. M. J. de Groot, E. H. Huizing, J. E. Veldman and G. F. Smoorenburg, *Hear. Res.*, 2000, **144**, 147–156.
36 C. Generotti, B. C. Cox, J. Singh, D. Hamilton, E. McKenzie, B. W. O'Malley Jr and D. Li, *Sci. Rep.*, 2022, **12**, 18032.
37 S. A. Lajud, Z. Han, F.-L. Chi, R. Gu, D. A. Nagda, O. Bezpalko, S. Sanyal, A. Bur, Z. Han, B. W. O'Malley Jr and D. Li, *J. Controlled Release*, 2013, **166**, 268–276.
38 S. A. Lajud, D. A. Nagda, P. Qiao, N. Tanaka, A. Civantos, R. Gu, Z. Cheng, A. Tsourkas, B. W. O'Malley Jr and D. Li, *Otol. Neurotol.*, 2015, **36**, 341–347.
39 M. N. Kayyalia, J. R. A. Wooltortona, A. J. Ramseya, M. Lin, T. N. Chao, A. Tsourkas, B. W. O'Malley Jr and D. Li, *J. Controlled Release*, 2018, **279**, 243–250.